Amino acid transporter Asc-1 (SLC7A10) expression is altered in basal ganglia in experimental Parkinsonism and L-dopa-induced dyskinesia model mice

Kazuki Nakahara[1], Hiroaki Okuda[2], Ayami Isonishi[1], Yoshie Kawabe[1], Tatsuhide Tanaka[1], Kouko Tatsumi[1], Akio Wanaka[1]

[1]Department of Anatomy and Neuroscience, Faculty of Medicine, Nara Medical University, Kashihara, Nara, Japan

[2]Department of Anatomy, Graduate School of Medical Science, Kanazawa University, Kanazawa, Ishikawa, Japan

Corresponding author: Kouko Tatsumi

E-mail: radha815@naramed-u.ac.jp

Abstract

In Parkinson's disease (PD), a decrease in dopamine levels in the striatum causes abnormal circuit activity in the basal ganglia, resulting in increased output via the substantia nigra pars reticulata (SNr). A characteristic feature of glutamatergic synaptic transmission in the basal ganglia circuitry under conditions of dopamine depletion is enhanced synaptic activity of NMDA receptors. However, the cause of this NMDA receptor hyperactivity is not fully understood. We focused on Asc-1 (SLC7A10), an alanine–serine–cysteine transporter, as one of the factors that regulate NMDA receptor activity by modulating D-serine and glycine concentration in synaptic clefts. We generated PD model mice by injection of 6-hydroxydopamine into the unilateral medial forebrain bundle and analyzed the expression level of Asc-1 mRNA in the nuclei of basal ganglia (the external segment of the globus pallidus (GPe), subthalamic nucleus (STN), and SNr) compared to control mice. Each nucleus was dissected using laser microdissection, and RNA was extracted and quantified by quantitative PCR. Asc-1 mRNA expression was significantly higher in the GPe and lower in the SNr under the PD state than that in control naïve mice. The STN showed no change in Asc-1 mRNA expression. We further modeled L-dopa-induced dyskinesia by administering L-dopa continuously for 14 days to the PD model mice and found that Asc-1 mRNA expression in the GPe and SNr became close to that of control mice, regardless of the presence of abnormal involuntary movements. The present study revealed that Asc-1 mRNA expression is differentially regulated in the basal ganglionic nuclei in response to striatal dopamine concentration (depleted or replenished) and suggests that Asc-1 can be a therapeutic target for the amelioration of motor symptoms of PD.

Introduction

Asc-1 (SLC7A10), also known as sodium-independent alanine–serine–cysteine transporter-1, transports D-serine and glycine with high affinity in cooperation with SLC3A2 (4F2 heavy chain) [1]. Asc-1 is widely distributed throughout the rodent brain and its distribution pattern is similar to that of D-serine [2]. Asc-1 knockout mice show symptoms such as tremor, ataxia, rigidity, and persistent myoclonus, a phenotype that has been proposed to reflect neuronal hyper excitability resulting from impaired synaptic clearance of D-serine [3,4]. When Asc-1 is stimulated at hippocampal CA1/CA3 synapses in aged rats, it activates NMDA receptors and enhances long-term potentiation of the synapses, by releasing D-serine from neurons [5]. These findings suggest that Asc-1 controls NMDA receptor activity by modulating D-serine concentration in synaptic clefts.

In Parkinson's disease (PD), dopaminergic neurons in the substantia nigra pars compacta (SNc) are degenerated, and reduced levels of dopamine (DA) in the striatum lead to abnormal circuit activity in the basal ganglia and to increased output from the substantia nigra pars reticulata (SNr). 6-OHDA, a dopaminergic neuron-specific toxin, impairs spontaneous locomotion when injected into the medial forebrain bundle that contains the nigrostriatal axons, mimicking human PD. Injection of NMDA receptor antagonists into the SNr of such 6-OHDA-treated PD model mice ameliorates impaired locomotion, suggesting that NMDA receptors, but not AMPA receptors, are a major responder in glutamatergic synapses [6]. The composition of NMDA receptor subunits is altered in the DA-depleted state, and this change may contribute to the hyperactivity of SNr neurons and impaired locomotion [6]. Taken together, these observations indicate that synaptic activities involving NMDA receptors are enhanced in DA-depleted basal

ganglia circuits, but the causes of this enhancement have not been fully elucidated.

In the present study, we made PD model mice by injecting 6-OHDA into the unilateral medial forebrain bundle and supplemented them with L-dopa. As is frequently observed in human PD patients, continuous L-dopa treatment causes dyskinesia (abnormal hyper locomotion). We focused on Asc-1 as one of the regulators of NMDA receptor activity and analyzed the changes of its gene expression levels over time under DA depletion (PD state) and at the onset of L-dopa-induced dyskinesia (LID). In addition to the SNr, we investigated the external segment of the globus pallidus (GPe) and the subthalamic nucleus (STN), which constitute the indirect pathway of the basal ganglia circuit. Although they mainly receive GABAergic inputs, they express NMDA receptors as well as GABA receptors in the normal state [7]. We dissected out the GPe, STN, and SNr from brain sections in an area-specific manner by laser microdissection and measured Asc-1 mRNA expression by quantitative PCR. Asc-1 mRNA expression was significantly higher in the GPe and significantly lower in the SNr under the PD state than that in control naïve mice (without 6-OHDA treatment). On the other hand, Asc-1 mRNA expression in the treated STN was comparable to that in the control mice. The present study demonstrates novel changes in synapses in the basal ganglia associated with DA depletion, and that these changes can be resolved by DA supplementation. Our results suggest that the Asc-1 can be a new therapeutic target to control motor deficits in PD.

Materials and Methods

Animals

Forty adult male C57BL/6 mice (~12 weeks old, 28–32 g body weight before the operation) were used. These mice were housed in standard cages with access to food, and all protocols for the animal experiments were approved by the Animal Care Committee of Nara Medical University in accordance with the policies established in the NIH Guide for the Care and Use of Laboratory Animals.

Experimental design

Fig. 2 illustrates the experimental schedules. In experiment 1, vehicle (0.02% ascorbic acid; FUJIFILM Wako, dissolved in saline) or 6-hydroxydopamine hydrobromide (6-OHDA; Merck Millipore, dissolved in vehicle at the concentration of 15 mg/ml, drug weight includes salt (hydrobromide) weight, hereafter weight of drug includes salt weight unless otherwise stated) was injected unilaterally to the medial forebrain bundle (detailed procedures are described below). The brains were removed and quickly frozen on day 21 after injection.

In experiment 2, vehicle or 6-OHDA was injected as in experiment 1. We next selected mice showing significant motor impairment in a cylinder test (details are described below) on day 21 in the 6-OHDA-injected group. Selected mice were divided into the following groups; PD + saline group: mice received injections of saline daily for 14 days (day 21 to day 34) and sacrificed on day 34; LID-on group: mice received injections of L-dopa (20 mg/kg, i.p., Dopaston; Ohara Pharmaceutical) daily for 14 days and sacrificed in 60 min after the last L-dopa dose on day 34; LID-off group: mice received injections

of L-dopa as with the LID-on group and sacrificed on 24 h after the last L-dopa dose later (day 35)(for details, see Fig. 4a in the Results). On day 34, abnormal involuntary movements (AIMs) scores were measured to confirm the presence of dyskinesia behavior (details to follow). In the Control + saline group, mice were injected with vehicle instead of 6-OHDA and received injections of saline daily for 14 days. The brains of each group were removed and quickly frozen.

Vehicle or 6-OHDA injection

Injection into the median forebrain bundle was done according to standard methods [8,9,12] with some modifications. Briefly, 30 min before vehicle or 6-OHDA injection, a mixture of desipramine hydrochloride (25 mg/kg, i.p., FUJIFILM Wako) and pargyline hydrochloride (5 mg/kg, i.p., Merck Millipore) was administered to increase the selectivity of 6-OHDA-induced lesion. Each mouse was then anesthetized with a mixture of medetomidine hydrochloride (0.75 mg/kg, Domitor Nippon Zenyaku Kogyo), midazolam (10 mg/Kg, Dormicum, Astellas Pharma), and butorphanol tartrate (0.75 mg/kg, Vetorphale, Meiji Seika Kaisha) [10]. Vehicle and 6-OHDA were freshly prepared before each surgery. A Hamilton syringe (Neuro Syringe 7001) was inserted into the left median forebrain bundle at the following coordinates, according to the mouse brain atlas [11]: Bregma posterior 1.2 mm, lateral 1.1 mm, and ventral 5.0 mm. Vehicle or 6-OHDA was then injected (0.2 µl, at 0.1 µl/min) with a microinjector (IMS-30, Narishige Scientific).

The body weight of 6-OHDA-injected mice was monitored post-injection because this group of mice was debilitated due to dehydration and malnutrition, and some of them died. To prevent death by treatment, the mice received 1.0 ml of 4% glucose–saline

136 solution subcutaneously twice daily and were fed with glucose–saline jelly and chocolate
137 for 10 days after surgery.
138
139 **Behavioral tests**
140 A cylinder test was performed by standard methods [12,13] to evaluate unilateral 6-
141 OHDA on day 21 (Fig. 2, Experiment 2). In brief, mice were placed individually in a clear
142 acrylic cylinder (80 mm diameter and 150 mm height) and a video was recorded for 5
143 min without previous habituation. The number of contacts with their right or left forelimb
144 was counted. A limb use asymmetry score was calculated based on the number of wall
145 contacts performed with the right forelimb as a percentage of the total wall contacts.
146 On day 34, mice were scored based on the AIMs scale [14,15] with some
147 modifications. Briefly, AIMs were classified into locomotive, axial, and limb subtypes
148 and scored on a severity scale from 0 to 4 (0, absent; 1, occasional; 2, frequent; 3,
149 continuous; 4, continuous and not interruptible by outer stimuli). After L-dopa treatment,
150 mice were placed in individual cages and dyskinesia behaviors were assessed by AIMs
151 scale every 20 min, for 1 min, over a period of 140 min.
152
153 **Tissue Preparation and immunohistochemistry**
154 Mice were perfused with 4% paraformaldehyde (PFA) in phosphate-buffered saline
155 (PBS). Brains were removed and post-fixed in 4% PFA, and cryopreserved in 30%
156 sucrose until they sank, and cryosections were cut to 40-μm thickness on a cryostat (Leica
157 CM1860, Leica Microsystems). Sections were used for immunohistochemistry study and *in*
158 *situ* hybridization.

All histological procedures were performed as described previously [7]. For primary antibody, anti-Slc7a10 (N-terminal) (1:400, rabbit polyclonal, GeneTex) and anti-tyrosine hydroxylase (TH; 1:100,000, mouse monoclonal, ImmunoStar) [16–18] antibodies were employed. The specificity of the anti-Slc7a10 antibody was verified by the absence of staining with antibody pre-absorbed with antigen [15]. We used anti-rabbit or -mouse IgG combined with amino acid polymers and peroxidase (Histofine Simple Stain MAX PO (R), MAX PO (M) Kit, respectively, Nichirei Bioscience) for secondary antibodies. The peroxidase color reaction was performed in diaminobenzidine tetrahydrochloride (DAB) solution (DAB Substrate Kit, Vector Laboratories).

In situ hybridization

Partial cDNA for mouse SLC7A10 was amplified from adult mouse brain total RNA by reverse transcriptase-PCR using the following primers: forward primer: partial forward primer, 5′-GTGAACAGCTCCAGCGTACG-3′ (NCBI Reference Sequence: NM_017394.4, complement of nucleotides (nt) 638–657); partial reverse primer, 5′-CAGCGTCTGACATGAATCATGG-3′ (reverse complement of nt 1179–1200). Digoxigenin (DIG) -labeled RNA probes were prepared using an RNA labeling mixture (Roche Diagnostics) and a T7 or SP6 RNA polymerase (Roche Diagnostics) according to the manufacturer's instructions. *In situ* hybridization was carried out as previously described [19]. Briefly, free-floating sections were treated with 0.75% glycine in PBS for 15 min twice, 0.3% Triton X-100 in PBS for 20 min, 1mM ethylenediaminetetraacetic acid (EDTA) (pH 8.0) for 15 min at 97 °C, and acetylated by 0.25% acetic anhydride in 0.1 M triethanolamine for 10 min. Then, sections were incubated hybridization buffer

containing 1.0 μg/mL DIG -labeled probes at 60 °C overnight. Next day, sections were sequentially treated in 2x saline sodium citrate (SSC; 1× SSC = 0.15 M NaCl, 0.015 M $Na_3C_6H_5O_7 \cdot 2H_2O$) /50% formamide/0.1% *N*-lauroylsarcosine (NLS) for 15 min at 60 °C twice, RNase buffer (10 mM Tris-HCl, pH 8.0, 1 mM EDTA, 500 mM NaCl) containing 20 μg/mL RNase A (Sigma-Aldrich) for 30 min at 37 °C, 2× SSC/0.1% NLS for 15 min twice, 0.2× SSC/0.1% NLS twice. The hybridized probe was detected with an alkaline phosphatase–conjugated anti-DIG antibody (1:1000, sheep polyclonal, Roche Diagnostics). Alkaline phosphatase activity was visualized by nitroblue tetrazolium (NBT) and 5-bromo-4-chloro-3-indolyl phosphate (BCIP) (Roche Diagnostics).

Western blot analysis

To evaluate the efficacy of 6-OHDA lesion, we performed western blot analysis as previously described [20]. The primary antibodies used were TH (1:5,000, rabbit polyclonal, Merck Millipore) and glyceraldehyde-3-phosphate dehydrogenase (GAPDH; 1:10,000, mouse monoclonal, Merck Millipore). Immunodetection was performed using a chemiluminescence kit (Immunostar LD and Zeta, Wako Chemical) with horseradish peroxidase-conjugated antibody against rabbit IgG (1:10,000, Cell Signaling Technology) or against mouse IgG (1:10,000, Cell Signaling Technology) according to the manufacturer's instructions.

Laser microdissection

Tissue preparation was performed as described in a previous report [7] with some modifications. In brief, mouse brains were removed after cervical dislocation and immediately frozen. Coronal sections containing the GPe (Bregma -0.58 to -0.94), STN

(Bregma -1.7 to 2.3), and SNr (Bregma -3.16 to -3.64) were cut at 25-μm thickness on a cryostat (Leica CM1860, Leica Microsystems). Sections with 100-μm intervals were mounted on a PEN membrane slide (Leica Microsystems). The slides were immediately dried and fixed in cold ethanol/acetic acid (19:1) for 60 s. To identify the GPe, STN, and SNr, tissues on slides were stained with 0.5% thionin acetate solution (Merck Millipore) dissolved in 66.32 mM sodium acetate for 30 s. They were then washed in sterile-filtered water treated with diethyl pyrocarbonate (DEPC, Nacalai Tesque), washed with RNase-free distilled water (Thermo Fisher) for 60 s, and immediately dried by a hair dryer. We dissected out the GPes, STNs, and SNrs from 10–12 sections per mouse using an LMD 6500 system (Leica Microsystems) and subjected them to RNA extraction.

RT-qPCR

Total RNA was isolated from each nucleus using a PicoPure RNA Isolation Kit (Arcturus) according to manufacturer's instruction. For cDNA synthesis, we used a 1st strand cDNA synthesis kit (Takara Bio). RT-qPCR was performed on a Thermal Cycler Dice (Takara Bio) with the following primer sets: Asc-1 (slc7a10) forward primer, 5'-AAGCTGCTGGGCTACTTTTC-3', reverse primer, 5'-ATGAATCATGGGCCAGGAAGC-3'; GAPDH forward primer5'-AACGACCCCTTCATTGACCTC -3', reverse primer, 5'-ACTGTGCCGTTGAATTTGCC -3'. A 2 μL volume of cDNA was used as the PCR template in 20 μL of reaction mixture containing two primers (5 μM each), 10 μL of SYBR qPCR mix (TOYOBO). Optimal amplification cycles were 24 cycles for Asc-1 gene. The amplified products were separated in 2% agarose gels and visualized by

231 ethidium bromide staining and subsequent UV irradiation.

232

233 **Statistics**

234 Statistical analyses were performed using Student's t-test or one-way analysis of variance

235 (ANOVA) followed by the Games-Howell post hoc test using Microsoft Excel software

236 (Microsoft, ver. 2013) or the IBM Statistical Package for Social Science (SPSS v23). All

237 data are expressed as means ± SEM. The significance level was set at $p < 0.05$.

Results

Immunohistochemical analysis showed widespread distribution of Asc-1 immunoreactivity in the mouse brain (**Fig. 1A**). Consistent with a previous report [2], Asc-1 was strongly expressed in the brainstem, as well as in the midbrain and basal forebrain. In addition to the GPe, in which we previously reported Asc-1 expression [15], we focused on other nuclei constituting the basal ganglia circuit. The STN and SNr also showed strong immunoreactivity (**Fig. 1A and B**). *In situ* hybridization analysis confirmed that Asc-1 mRNA is also expressed in these nuclei, indicating parallel protein and mRNA expression for Asc-1 (**Fig. 1C**).

To examine changes in Asc-1 mRNA expression in response to DA depletion, we generated a PD model mouse by unilaterally injecting 6-OHDA into the left MFB. The control group received vehicle injection instead of 6-OHDA (**Fig. 2**, Experiment 1). Twenty-one days after 6-OHDA injection (day 21), dopaminergic axons in the striatum (the target of the nigrostriatal tract) were almost completely degenerated, as confirmed by immunostaining of TH (**Fig. 3A**) and by Western blotting (**Fig. 3B**). The GPe, STN and SNr were dissected out by laser microdissection from Nissl-stained brain sections of PD model and control mice (**Fig. 3C**). Although the mouse STN is very small among these three nuclei, laser microdissection allowed us to isolate this nucleus specifically and reproducibly. We extracted mRNA samples from dissected nuclei, and Asc-1 mRNA was measured by qPCR. On day 21, when the nigrostriatal dopaminergic axons were completely degenerated, the mRNA expression became significantly higher than the control group in the GPe ($p=0.002$, Student's t-test, control group: $n=6$, 6-OHDA group: $n=7$) (**Fig. 3D**). In clear contrast to the GPe, there was no significant difference in Asc-1

mRNA expression between the 6-OHDA and control groups in the STN p=0.63, Student's t-test, control group: n=6; 6-OHDA group: n=6) (**Fig. 3E**). The SNr in the 6-OHDA group showed significantly lower expression compared to the control group (p=0.0002, Student's t-test, control group: n=6; 6-OHDA group: n=6) (**Fig. 3F**).

The current standard therapy for PD is dopamine replacement using L-dopa, a blood–brain barrier-permeable dopamine precursor [21]. Chronic L-dopa treatment produces AIMs known as L-dopa-induced dyskinesia (LID) as a side effect. We next investigated whether L-dopa treatment affects the expression of Asc-1 mRNA in the PD model mice. PD model mice were treated daily for 14 days with L-dopa to induce LID (**Fig. 2**, Experiment 2). On day 34, AIM scores were measured, and, consistent with previous reports [11], the scores peaked at 60 min after L-dopa administration (LID-ON state) and dyskinesia-like behaviors were no longer observed after 140 min (LID-OFF state) (**Fig. 4A**). Brain samples were collected by laser microdissection at 60 min after the last L-dopa dose on day 34 and 24 h later (day 35). The regions of interest were the GPe and SNr, both of which exhibited changes in Asc-1 mRNA expression induced by PD pathology in the Experiment 1. Treatment with saline for 14 consecutive days did not eliminate the significant increase in Asc-1 expression in the Gpe (Fig.4B, control vs PD group, p=0.002) and the decrease in the SNr (Fig. 4C, control vs PD group, p=0.037). These results showed that the significant change of Asc-1 mRNA expression level in the Gpe and the SNr continued for at least 14 days after degeneration of nigrostriatal tract. In contrast, continuous administration of L-Dopa tended to resolve the changes in Asc-1 expression in both nuclei (Fig. 4B and 4C). There was no significant difference in Asc-1 mRNA expression in the presence or absence (LID-ON/OFF) of dyskinesia-like behavior in either the GPe or the SNr (**Fig. 4B and C**).

Discussion

The present study revealed that the GPe and STN, which constitute the indirect pathway of the basal ganglia circuit, responded differently to degeneration of DA neurons: Asc-1 mRNA increased in the GPe, but did not change in the STN. The SNr, one of the output nuclei of the basal ganglia circuit, exhibited decreased Asc-1 mRNA expression in response to DA depletion. The changes in the GPe and SNr tended to be resolved by DA replacement with continuous L-dopa administration regardless of the presence of AIMs.

Accumulating evidence has drawn attention to the electrophysiological properties of the GPe in impaired motor functions in PD [22–24]. There are two major types of GABAergic projection neurons in the GPe, namely, prototypical and arkypallidal neurons [25], of which prototypical neurons fire rapidly in vivo, express parvalbumin, and project preferentially to the STN. These neurons express NMDA receptors containing GluN2C as their NR2 subunit [26]. Among the NMDA receptor subunits, GluN2C has unique pharmacological properties: low sensitivity to Mg2+ blockade, high glutamate affinity, and no desensitization [27]. Taking these into account, NMDA receptors expressed by the prototypical neurons may contribute to the tonic excitatory bursts in the GPe. Indeed, specific pharmacological enhancement of NMDA receptors containing GluN2C in the GPe increased the firing of GPe neurons and alleviated motor deficits of PD model mice [28]. In line with this, increased Asc-1 mRNA expression in the GPe of PD model mice (Fig. 3D) may lead to enhanced uptake of D-serine and glycine from synaptic clefts and then to decreased NMDA receptor activity. In this case, Asc-1 would exert adverse effects on motor function. An alternative and opposite explanation, however, is possible: DA depletion may reduce NMDA receptor activity for some reason, and Asc-1 may increase

311 to active NMDA receptor by releasing D-serine to synaptic clefts as an antiporter [5]. The
312 increased expression of Asc-1 mRNA may reflect altered transmission at excitatory
313 synapses. In view of the concept of the tripartite synapse, the possibility that astrocytes
314 are involved in this change in synaptic transmission cannot be ignored. We have reported
315 that Olig2-lineage astrocyte (Olig2-AS) [29], a subpopulation of astrocytes abundant in
316 the basal ganglia, expresses Asc-1 mRNA in the Gpe [15]. Olig2-AS-derived Asc-1
317 mRNA may contribute to the increased Asc-1 expression under PD state. In this study, it
318 was not clear whether the increased Asc-1 mRNA expression was of neuronal or
319 astrocytic origin, but it will be interesting to see how Olig2-AS are involved under PD
320 conditions, which will be the subject of our future study.
321 DA depletion increases NMDA receptors in the SNr, but does not change AMPA
322 receptor-mediated spontaneous and evoked excitatory postsynaptic currents [6].
323 Microinjection of NMDA receptor antagonists into the SNr of PD model mice results in
324 significant improvement of spontaneous locomotion [6]. The function of NMDA
325 receptors containing either GluN2B or GluN2D subunits is dramatically reduced in the
326 PD model mice, while the function of heteromeric NMDA receptors that contain GluN2A
327 is maintained [6]. Such changes in the subunit composition of NMDA receptors may
328 contribute to the hyperactivity of SNr neurons and to impaired locomotion in the DA-
329 depleted state. In the present study, Asc-1 expression in the SNr was decreased upon DA
330 depletion, in clear contrast to that in the GPe. Downregulation of the Asc-1 transporter
331 may lead to excess amounts of D-serine and glycine in synaptic clefts and thereby
332 enhance the activities of NMDA receptors and of SNr neurons. When DA was
333 supplemented with continuous L-dopa administration, the increase or decrease in Asc-1
334 expression in both nuclei tended to be resolved, and this effect persisted regardless of the

ON/OFF state of LID. This suggests that Asc-1 mRNA expression in the Gpe and SNr may be under on/off control of DA rather than dose-dependent control. To delineate the regulatory mechanisms, we need to measure regional dopamine contents in the Gpe and SNr of PD, LID-ON and LID-OFF mice. L-dopa is an established treatment for movement disorders in PD, but its mechanism of action is not fully understood. It has been known that the serotonergic nervous system plays an important role in the conversion of L-dopa to DA [30], and abnormal serotonergic transmission is one of the reasons for the development of dyskinesia. L-dopa has a wide range of complex neurochemical effects beyond its conversion to DA in striatal dopaminergic neurons, including indirect effects on cholinergic, GABAergic and glutamatergic neurons, and its potential to be converted to bioactive metabolites independently of DA neurotransmission [31]. L-dopa administration may thus have complex impacts on altering Asc-1 mRNA expression.

The present study reveals novel changes of Asc-1 mRNA of the GPe and SNr, in synapses associated with DA depletion, and further shows that these changes can be normalized by dopamine replacement. Asc-1 may become a new therapeutic target to control motor deficits and L-dopa-induced abnormal motor activities in PD.

However, it remains to be clarified whether Asc-1 gene expression changes in the GPe and SNr are a cause or an effect of the PD pathology.

Funding

This work was supported by JSPS KAKENHI Grant Numbers JP19K06928 (to K.T.), JP19K16480 (to A.I.), JP19K07827 (to T.T.), and JP18K06836 (to A.W.).

References

[1] Y. Fukasawa, H. Segawa, J.Y. Kim, A. Chairoungdua, D.K. Kim, H. Matsuo, S.H. Cha, H. Endou, Y. Kanai, Identification and characterization of a NA+-independent neutral amino acid transporter that associates with the 4F2 heavy chain and exhibits substrate selectivity for small neutral D- and L-amino acids, J Biol Chem. 275 (2000) 9690–9698. https://doi.org/10.1074/jbc.275.13.9690.

[2] L. Helboe, J. Egebjerg, M. Møller, C. Thomsen, Distribution and pharmacology of alanine-serine-cysteine transporter 1 (asc-1) in rodent brain, Eur J Neurosci. 18 (2003) 2227–2238. https://doi.org/10.1046/j.1460-9568.2003.02966.x.

[3] X. Xie, T. Dumas, L. Tang, T. Brennan, T. Reeder, W. Thomas, R.D. Klein, J. Flores, B.F. O'Hara, H.C. Heller, P. Franken, Lack of the alanine-serine-cysteine transporter 1 causes tremors, seizures, and early postnatal death in mice, Brain Res. 1052 (2005) 212–221. https://doi.org/10.1016/j.brainres.2005.06.039.

[4] A.R. Rutter, R.L. Fradley, E.M. Garrett, K.L. Chapman, J.M. Lawrence, T.W. Rosahl, S. Patel, Evidence from gene knockout studies implicates Asc-1 as the primary transporter mediating D-serine reuptake in the mouse CNS, Eur J Neurosci. 25 (2007) 1757–1766. https://doi.org/10.1111/j.1460-9568.2007.05446.x.

[5] J.M. Billard, T. Freret, Asc-1 transporter activation: an alternative to rescue age-related alterations in functional plasticity at rat hippocampal CA3/CA1 synapses, J Neurochem. 147 (2018) 514–525. https://doi.org/10.1111/jnc.14586.

[6] G. Sitzia, I. Mantas, X. Zhang, P. Svenningsson, K. Chergui, NMDA receptors

are altered in the substantia nigra pars reticulata and their blockade ameliorates motor deficits in experimental parkinsonism, Neuropharmacology. 174 (2020) 108136. https://doi.org/https://doi.org/10.1016/j.neuropharm.2020.108136.

[7] P. Ravenscroft, J. Brotchie, NMDA receptors in the basal ganglia, J Anat. 196 (2000) 577–585. https://doi.org/10.1017/S0021878299006597.

[8] H. Sano, A. Nambu, The effects of zonisamide on L-DOPA–induced dyskinesia in Parkinson's disease model mice, Neurochem Int. 124 (2019) 171–180. https://doi.org/10.1016/j.neuint.2019.01.011.

[9] I.D. Wahyu, S. Chiken, T. Hasegawa, H. Sano, A. Nambu, Abnormal cortico-basal ganglia neurotransmission in a mouse model of L-DOPA-induced dyskinesia, J Neurosci. 41 (2021) 2668–2683. https://doi.org/10.1523/JNEUROSCI.0267-20.2020.

[10] Y. Kirihara, M. Takechi, K. Kurosaki, Y. Kobayashi, T. Kurosawa, Anesthetic Effects of a Mixture of Medetomidine, Midazolam and Butorphanol in Two Strains of Mice, Exp Anim. 62 (2013) 173–180. https://doi.org/10.1538/expanim.62.173.

[11] G. Franklin, K. B. J., and Paxinos, The Mouse Brain in Stereotaxic Coordinates., San Diego, CA Acad Press. (1997).

[12] Q. Peng, S. Zhong, Y. Tan, W.Q. Zeng, J. Wang, C. Cheng, X. Yang, Y. Wu, X. Cao, Y. Xu, The Rodent Models of Dyskinesia and Their Behavioral Assessment, Front Neurol. 10 (2019) 1–11. https://doi.org/10.3389/fneur.2019.01016.

[13] H. Sano, A. Nambu, The effects of zonisamide on L-DOPA–induced dyskinesia in Parkinson's disease model mice, Neurochem Int. 124 (2019) 171–180. https://doi.org/10.1016/j.neuint.2019.01.011.

406 [14] I. Sebastianutto, N. Maslava, C.R. Hopkins, M.A. Cenci, Validation of an
407 improved scale for rating l-DOPA-induced dyskinesia in the mouse and effects of
408 specific dopamine receptor antagonists, Neurobiol Dis. 96 (2016) 156–170.
409 https://doi.org/https://doi.org/10.1016/j.nbd.2016.09.001.
410 [15] K. Tatsumi, K. Kinugawa, A. Isonishi, M. Kitabatake, H. Okuda, S. Takemura,
411 T. Tanaka, E. Mori, A. Wanaka, Olig2-astrocytes express neutral amino acid
412 transporter SLC7A10 (Asc-1) in the adult brain, Mol Brain. 14 (2021) 1–12.
413 https://doi.org/10.1186/s13041-021-00874-8.
414 [16] P. Kosillo, K.M. Ahmed, E.E. Aisenberg, V. Karalis, B.M. Roberts, S.J. Cragg,
415 H.S. Bateup, Dopamine neuron morphology and output are differentially
416 controlled by mTORC1 and mTORC2., Elife. 11 (2022).
417 https://doi.org/10.7554/eLife.75398.
418 [17] Y. Han, Y. Zhang, H. Kim, V.S. Grayson, V. Jovasevic, W. Ren, M. V Centeno,
419 A.L. Guedea, M.A.A. Meyer, Y. Wu, P. Gutruf, D.J. Surmeier, C. Gao, M.
420 Martina, A. V Apkarian, J.A. Rogers, J. Radulovic, Excitatory VTA to DH
421 projections provide a valence signal to memory circuits., Nat Commun. 11
422 (2020) 1466. https://doi.org/10.1038/s41467-020-15035-z.
423 [18] K. Farrell, A. Lak, A.B. Saleem, Midbrain dopamine neurons signal phasic and
424 ramping reward prediction error during goal-directed navigation., Cell Rep. 41
425 (2022) 111470. https://doi.org/10.1016/j.celrep.2022.111470.
426 [19] Y. Komatsu, A. Watakabe, T. Hashikawa, S. Tochitani, T. Yamamori, Retinol-
427 binding Protein Gene is Highly Expressed in Higher-order Association Areas of
428 the Primate Neocortex, Cereb Cortex. 15 (2005) 96–108.
429 https://doi.org/10.1093/cercor/bhh112.

[20] H. Okuda, K. Tatsumi, S. Morita-Takemura, K. Nakahara, K. Nochioka, T. Shinjo, Y. Terada, A. Wanaka, Hedgehog signaling modulates the release of gliotransmitters from cultured cerebellar astrocytes, Neurochem Res. 41 (2016) 278–289. https://doi.org/10.1007/s11064-015-1791-y.

[21] S. Fahn, Description of Parkinson's disease as a clinical syndrome., Ann N Y Acad Sci. 991 (2003) 1–14. https://doi.org/10.1111/j.1749-6632.2003.tb07458.x.

[22] D.J. Hegeman, E.S. Hong, V.M. Hernández, C.S. Chan, The external globus pallidus: progress and perspectives, Eur J Neurosci. 43 (2016) 1239–1265. https://doi.org/https://doi.org/10.1111/ejn.13196.

[23] A.H. Gittis, J.D. Berke, M.D. Bevan, C.S. Chan, N. Mallet, M.M. Morrow, R. Schmidt, New roles for the external globus pallidus in basal ganglia circuits and behavior., J Neurosci . 34 (2014) 15178–15183. https://doi.org/10.1523/JNEUROSCI.3252-14.2014.

[24] B. de la Crompe, A. Aristieta, A. Leblois, S. Elsherbiny, T. Boraud, N.P. Mallet, The globus pallidus orchestrates abnormal network dynamics in a model of Parkinsonism, Nat Commun. 11 (2020) 1–14. https://doi.org/10.1038/s41467-020-15352-3.

[25] N. Mallet, B.R. Micklem, P. Henny, M.T. Brown, C. Williams, J.P. Bolam, K.C. Nakamura, P.J. Magill, Dichotomous Organization of the External Globus Pallidus, Neuron. 74 (2012) 1075–1086. https://doi.org/https://doi.org/10.1016/j.neuron.2012.04.027.

[26] A. Ravikrishnan, P.J. Gandhi, G.P. Shelkar, J. Liu, R. Pavuluri, S.M. Dravid, Region-specific Expression of NMDA Receptor GluN2C Subunit in Parvalbumin-Positive Neurons and Astrocytes: Analysis of GluN2C Expression

using a Novel Reporter Model, Neuroscience. 380 (2018) 49–62. https://doi.org/10.1016/j.neuroscience.2018.03.011.

[27] S.F. Traynelis, L.P. Wollmuth, C.J. McBain, F.S. Menniti, K.M. Vance, K.K. Ogden, K.B. Hansen, H. Yuan, S.J. Myers, R. Dingledine, Glutamate Receptor Ion Channels: Structure, Regulation, and Function, Pharmacol Rev. 62 (2010) 405 LP – 496. https://doi.org/10.1124/pr.109.002451.

[28] J. Liu, G.P. Shelkar, L.P. Sarode, D.Y. Gawande, F. Zhao, R.P. Clausen, R.R. Ugale, S.M. Dravid, Facilitation of GluN2C-containing NMDA receptors in the external globus pallidus increases firing of fast spiking neurons and improves motor function in a hemiparkinsonian mouse model, Neurobiol Dis. 150 (2021) 105254. https://doi.org/10.1016/j.nbd.2021.105254.

[29] K. Tatsumi, A. Isonishi, M. Yamasaki, Y. Kawabe, S. Morita-Takemura, K. Nakahara, Y. Terada, T. Shinjo, H. Okuda, T. Tanaka, A. Wanaka, Olig2-Lineage astrocytes: A distinct subtype of astrocytes that differs from GFAP astrocytes, Front Neuroanat. 12 (2018) 1–17. https://doi.org/10.3389/fnana.2018.00008.

[30] P.A. Cheshire, D.R. Williams, Serotonergic involvement in levodopa-induced dyskinesias in Parkinson's disease, J Clin Neurosci. 19 (2012) 343–348. https://doi.org/https://doi.org/10.1016/j.jocn.2011.09.008.

[31] P. De Deurwaerdère, G. Di Giovanni, M.J. Millan, Expanding the repertoire of L-DOPA's actions: A comprehensive review of its functional neurochemistry, Prog Neurobiol. 151 (2017) 57–100. https://doi.org/https://doi.org/10.1016/j.pneurobio.2016.07.002.

Figure legends

Fig. 1 Expression of Asc-1 in mouse brain.

(A) Immunochemical analysis using anti-Asc-1 antibody shows that Asc-1 is strongly expressed in the brain stem, mesencephalon, and basal forebrain. In the basal ganglionic circuit, GPe, STN, and SNr show strong Asc-1 expression. (B) GPe, STN, and SNr are also labeled strongly by immunofluorescence using anti-Asc-1 antibody. (C) Asc-1 mRNA expression in the GPe, STN, and SNr is confirmed by *in situ* hybridization. No specific hybridization signals were observed with the sense probe. Insets show Asc-1 mRNA signals under higher magnification. Scale bars = 1 mm in A and B; 200 μm in C; 50 μm in inset of C. CPu: Caudo-Putamen, cp: Cerebral Peduncle.

Fig. 2 Schematic representation of experimental schedules.

See Materials and Methods for details.

Fig. 3 Asc-1 mRNA expression level is altered in the GPe and SNr, but not in the STN, in dopamine depletion mice.

(A, B) Dopamine projection in the nigrostriatal tract is completely degenerated on day 21 in 6-OHDA-injected mice, as confirmed by immunostaining of anti-tyrosine hydroxylase antibody (A) and Western blotting (B). (C) The GPe, STN, and SNr were dissected from brain sections counterstained with thionin by laser microdissection. The low-magnification images are sections after each neuronal nucleus has been dissected by laser

502 microdissection. Scale bar: 2.5 mm. (D) Asc-1 mRNA expression is significantly higher
503 in the GPe on day 21 than in the control group. (E) There is no difference of Asc-1
504 mRNA expression level in the STN between control and 6-OHDA groups. (F) In the
505 SNr, Asc-1 mRNA expression is significantly lower than in the control group. Graphical
506 data are presented as the mean ± SEM. Student's t-test was used to compare mean values
507 for unpaired data. *$p < 0.05$; n.s., not significant.
508
509
510 **Fig. 4** Dopamine replacement with L-dopa administration resolves the changes in ASC-
511 1 mRNA expression in the GPe and SNr.
512 (A) AIM scores peaked at 60 min after the last L-dopa administration, and dyskinesia-
513 like behavior was no longer observed after 140 min. (B) Asc-1 mRNA expression in the
514 6-OHDA-injected GPe decreased after continuous L-dopa treatment and showed levels
515 comparable to those in controls on day 34. There was no difference in Asc-1 mRNA
516 expression in the presence or absence of dyskinesia-like behavior (LID-ON/OFF). (C) In
517 the L-Dopa-treated SNr, Asc-1 mRNA expression increased to levels comparable to those
518 in controls. There were no significant differences between LID-ON and LID-OFF states.
519 Graphical data are presented as the mean ± SEM. One-way analysis of variance (ANOVA)
520 followed by the Games-Howell post hoc test was used. *$p < 0.05$; n.s., not significant.

Fig.1

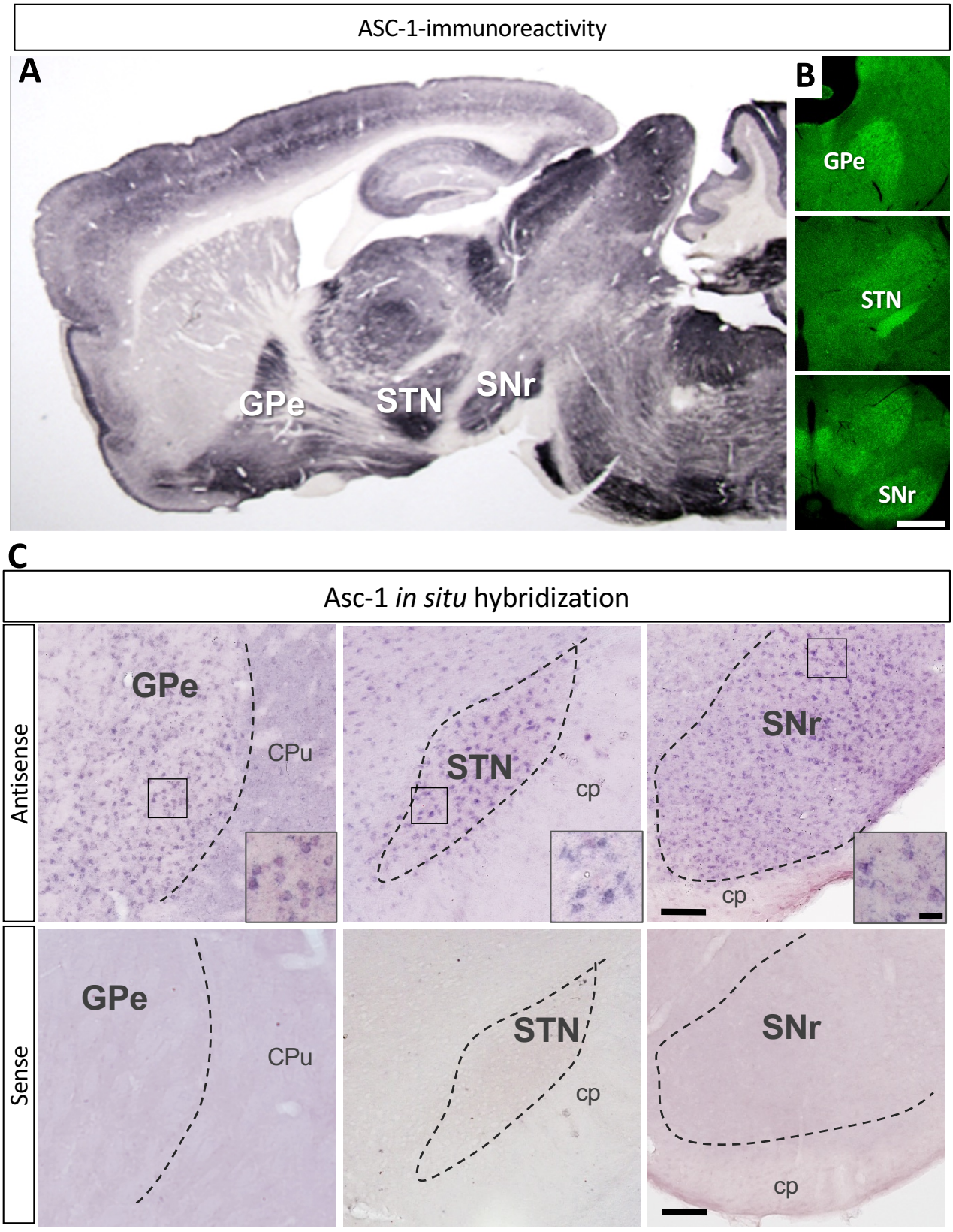
ASC-1-immunoreactivity
A
GPe
STN
SNr
B
GPe
STN
SNr
C
Asc-1 in situ hybridization
Antisense
GPe
CPu
STN
cp
SNr
cp
Sense
GPe
CPu
STN
cp
SNr
cp

Fig.2

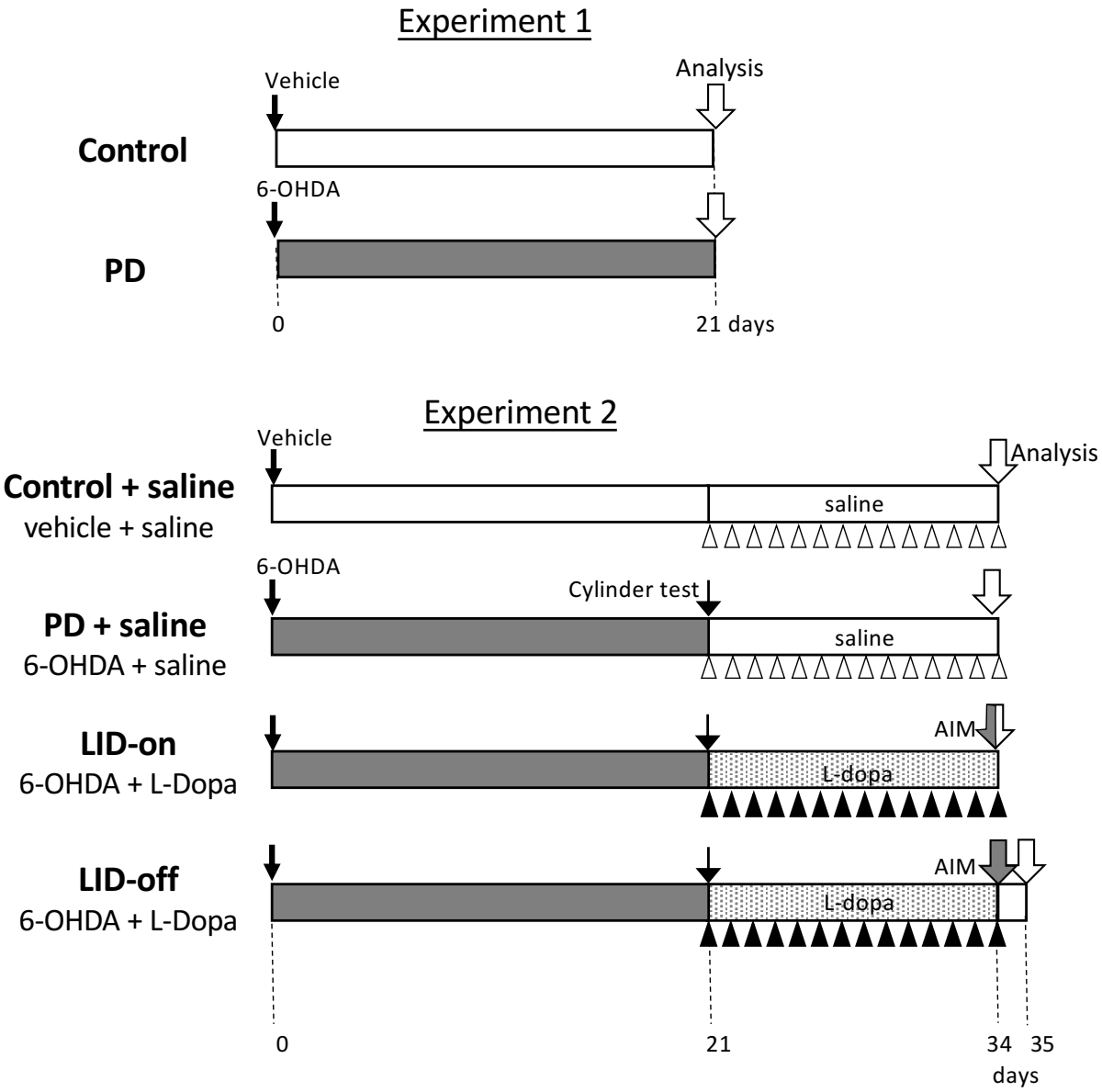
Experiment 1
Vehicle
Analysis
Control
6-OHDA
PD
0
21 days
Experiment 2
Vehicle
Analysis
Control + saline
vehicle + saline
saline
6-OHDA
Cylinder test
PD + saline
6-OHDA + saline
saline
AIM
LID-on
6-OHDA + L-Dopa
L-dopa
AIM
LID-off
6-OHDA + L-Dopa
L-dopa
0
21
34
35
days

Fig. 3

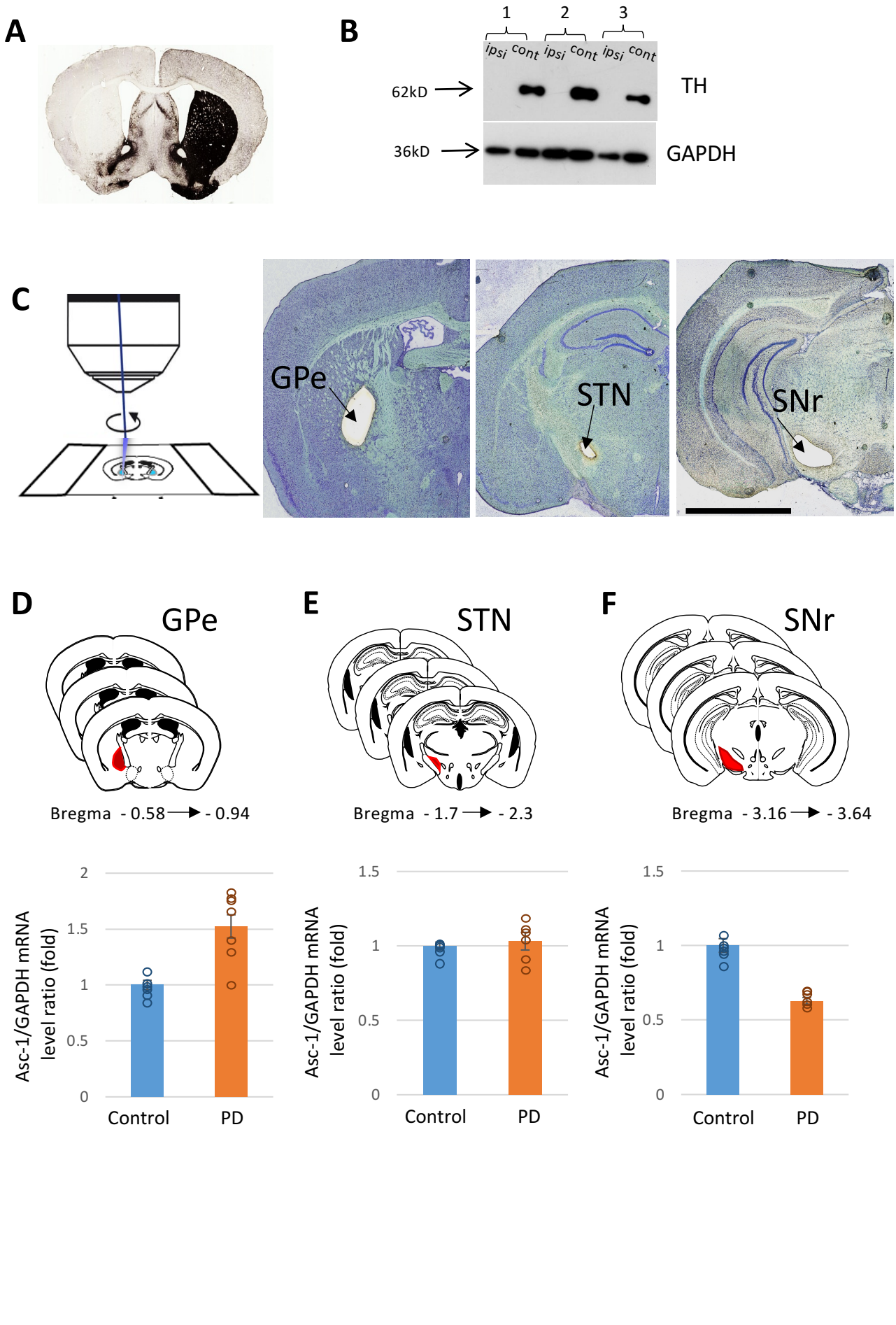
A
B
1
2
3
ipsi
cont
ipsi
cont
ipsi
cont
62kD
TH
36kD
GAPDH
C
GPe
STN
SNr
D
GPe
Bregma - 0.58 → - 0.94
E
STN
Bregma - 1.7 → - 2.3
F
SNr
Bregma - 3.16 → - 3.64
Asc-1/GAPDH mRNA level ratio (fold)
2
1.5
1
0.5
0
Control
PD
Asc-1/GAPDH mRNA level ratio (fold)
1.5
1
0.5
0
Control
PD
Asc-1/GAPDH mRNA level ratio (fold)
1.5
1
0.5
0
Control
PD

Fig. 4

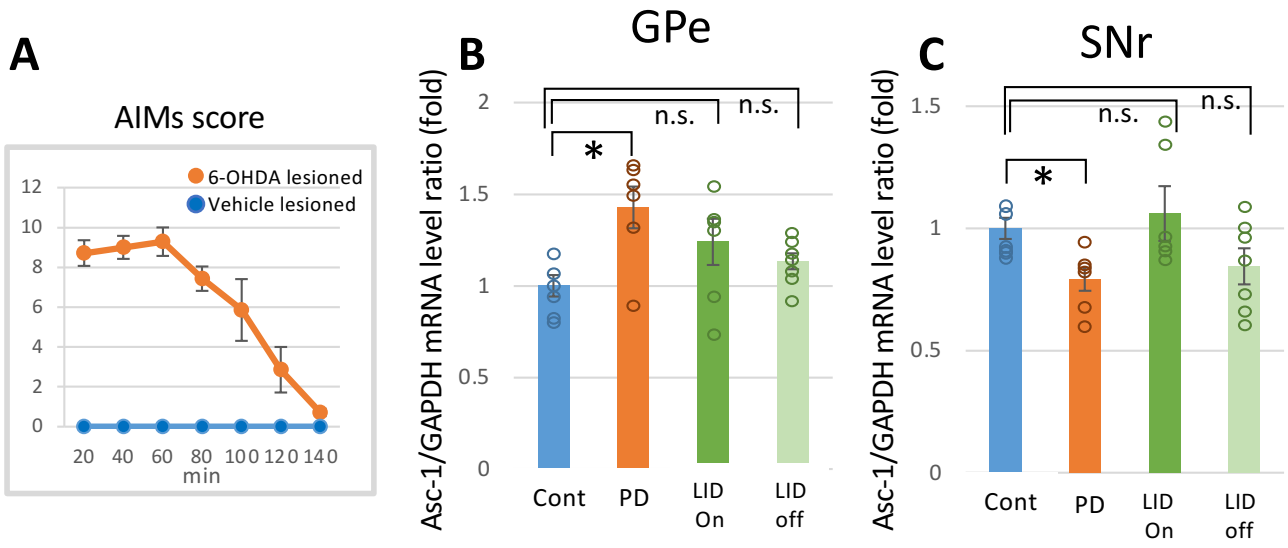
A
AIMs score
6-OHDA lesioned
Vehicle lesioned
12
10
8
6
4
2
0
20 40 60 80 100 120 140
min
B
GPe
Asc-1/GAPDH mRNA level ratio (fold)
2
1.5
1
0.5
0
n.s.
n.s.
*
Cont
PD
LID On
LID off
C
SNr
Asc-1/GAPDH mRNA level ratio (fold)
1.5
1
0.5
0
n.s.
n.s.
*
Cont
PD
LID On
LID off